ball, Jr. Concrete Median Barrier Research: Volume 2--Research Report. Federal Highway Administration, U.S. Department of Transportation, Rept. FHWA-RD-77-4, March 1976.
9. M. E. Bronstad and J. D. Michie. Recommended Procedures for Vehicular Crash Testing of Highway Appurtenances. NCHRP, Rept. 153, 1974.
10. Recommended Procedures for Vehicular Crash Testing of Highway Appurtenances. TRB, Transportation Research Circular 191, Feb. 1978.
11. R. N. Field and J. L. Beaton. Final Report of Full-Scale Dynamic Tests of Bridge Curbs and Rails. Materials and Research Department, California Department of Public Works, Sacramento, Aug. 30, 1957.

Publication of this paper sponsored by Committee on Safety Appurtenances.

Notice: The Transportation Research Board does not endorse products or manufacturers. Manufacturers' names are included in this paper because they are considered essential to its object.

Portable Concrete Median Barriers: Structural Design and Dynamic Performance

DON L. IVEY, HAYES E. ROSS, TEDDY J. HIRSCH, C. EUGENE BUTH, AND ROBERT M. OLSON

Types of portable concrete median barriers (CMBs) in use in the United States are described primarily in terms of structural details and the load-bearing characteristics of their end connections. Twelve end-connection designs are analyzed to produce estimates of their resistance to loads in four test conditions: simple tension, shear, yaw moment, and torsion. Rotational connection slack is estimated from the geometric properties of the different end connections. Nine crash tests conducted by four research agencies are examined. These tests cover a range of barrier lengths from 3.81 to 9.14 m (12.5-30 ft) and a range of connection details that vary from low to significant load capacity. The crash tests vary in intensity from a 7° test at 104.6 km/h (65 miles/h) to a 25° test at 99.8 km/h (62 miles/h). Analysis of these tests yields specific conclusions on the performance of CMBs. An energy analysis of portable CMBs during vehicle impacts is presented. Estimates of barrier deflection derived from this analysis check closely with deflections observed during crash tests. A parametric study of the influence of various barrier characteristics, including barrier length and mass, connection slack and strength, and support media static and sliding friction, is also presented. Based on this analysis, portable CMBs can now be designed to provide specific performance characteristics.

The most widely used class of construction-zone barriers with positive redirection characteristics is the portable concrete median barrier (CMB). There are at least as many variations in CMB design as there are states in which it is used. The CMB usually has no mechanical fastening to the ground but relies on mass and sliding friction for translational stability. It is always segmented, and segment lengths vary from 3.05 to 9.14 m (10-30 ft). Segment lengths of 3.05, 3.66, 3.81, 6.10, and 9.14 m (10, 12, 12.5, 15, 20, and 30 ft) have been used. It is in the method of joining these segments that there is the greatest variation.

Figures 1 and 2 show applications of the portable CMB in Virginia and Texas, respectively. In Virginia, the barrier segments are 3.66 m long with a vertical concrete shear key connection design. In Texas, the segments are 9.14 m long, and three no. 8 reinforcing bar dowels form the connection. These two connections and four other representative connections are shown in Figures 3-8. Although only 6 connection designs are shown, 12 have been identified. Of these 12, 5 are variations of the California vertical pin connection shown in Figure 7.

The evolution of the portable CMB was straightforward. The CMB was first produced by forming the barrier in place for a permanent installation. Then, in an effort to reduce costs, precast fabrication was used. This made it necessary to move barrier segments from place to place. It became obvious that barrier segments could be placed temporarily in construction zones before final placement as permanent barriers. Once this was recognized, the use of portable CMBs became widespread. In early applications, the functional characteristics of the barrier were assumed to be adequate, an assumption that has generally been borne out by field experience.

TEST RESULTS

As the use of the CMB became more widespread, it was subjected to testing by at least four organizations: Southwest Research Institute (SwRI) (1), the Texas Transportation Institute (TTI) (2), the New York Department of Transportation (NYSDOT), and the California Department of Transportation (Caltrans) (3).

Currently, a total of nine tests have been conducted on barriers that may be considered portable. The results of these tests are summarized in Table 1. In six of the tests, the results were successful at least from the consideration of structural capacity [it must be noted that the test of a 2041-kg (4500-lb) vehicle at 96.5 km/h (60 miles/h) and 25° is a test of structural adequacy, not a test of vehicle reaction from a safety standpoint]. At least three designs have been shown to perform adequately in regard to structural integrity under vehicle collisions at the 96.5-km/h, 25°, 2041-kg energy level. This performance is illustrated in SwRI test CMB-24, TTI test CMB-2, and New York test NY-1. Barrier-segment lengths were 6.10 m (20 ft) for the New York and SwRI tests and 9.14 m (30 ft) for the TTI test. Structural failures occurred in SwRI test CMB-18, where the longitudinal reinforcement of the main section was insufficient to prevent a large portion of one segment from being dislodged; Caltrans test 292, where a main barrier segment was broken; and Caltrans test 293, where one barrier segment was knocked over. As a result of these latter two tests, Caltrans upgraded the design to the one shown in Figure 5 and described in Table 2.

Although many of these tests showed adequate barrier performance, there are a variety of untested designs in use. Some of these are of significantly

Figure 1. Portable CMB in Virginia.

Figure 2. Portable CMB in Texas.

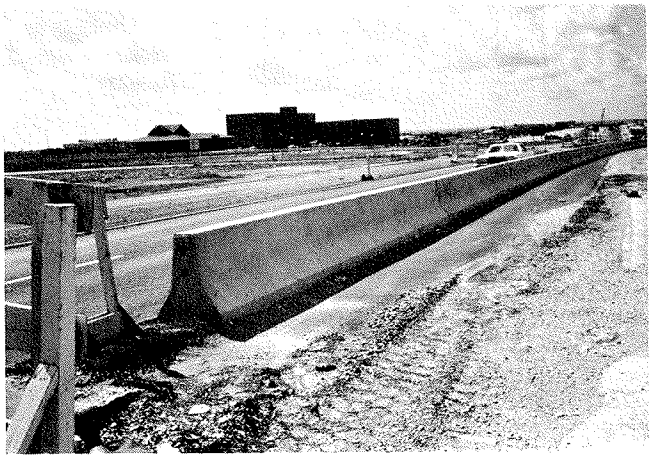

lower strength than the designs tested. In an effort to gain some perspective on the different barrier-connection designs that are in use, 12 designs were subjected to a simple structural analysis. This analysis consisted of determining the ultimate strength of the barrier connection under four loading conditions.

Figure 9 shows a coordinate system used to define these loads. In this system, the x coordinate is coincident with the longitudinal barrier centroidal axis. The y coordinate is vertical and the z coordinate is perpendicular to the longitudinal barrier axis and parallel to the ground plane. The origin of coordinates is at the cross-section center of gravity at a barrier segment joint. The four loading conditions analyzed are the ultimate tensile strength (P), a tensile force in the x direction; the ultimate shear strength (V), the shear in the z direction; the ultimate moment (M), the moment about the y axis; and the ultimate resistance to torsion (T), a torque about the x axis. Each of these ultimate strengths is the strength of the connection, not the strength of the barrier cross section.

Table 2 gives the results of these computations. The various designs are listed sequentially, from the strongest connections to the weakest. The final column in the table denotes the other connection property--i.e., how much one segment of the barrier may rotate with respect to an adjacent segment before significant moment begins to develop about the y axis. In general, the lower the value of the connection slack, the better the barrier performance should be. Stated another way, the lower this value, the lower should be the barrier deflection under a specific impact condition. It seems apparent from Table 2 that a variety of designs with different performance characteristics are represented.

The following performance levels of barriers are considered, based on the amount of kinetic energy associated with the lateral component of vehicle velocity (1 mile = 1.6 km; 1 lb = 0.45 kg):

Figure 3. Virginia vertical tongue-groove connection.

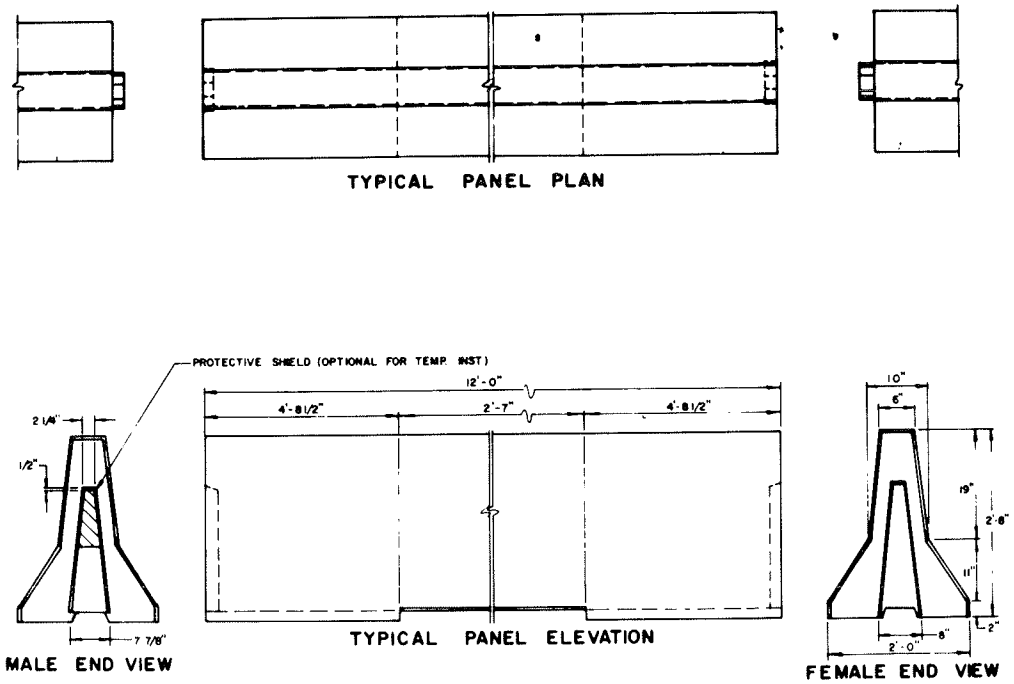

Figure 4. Colorado top hook and rebar.

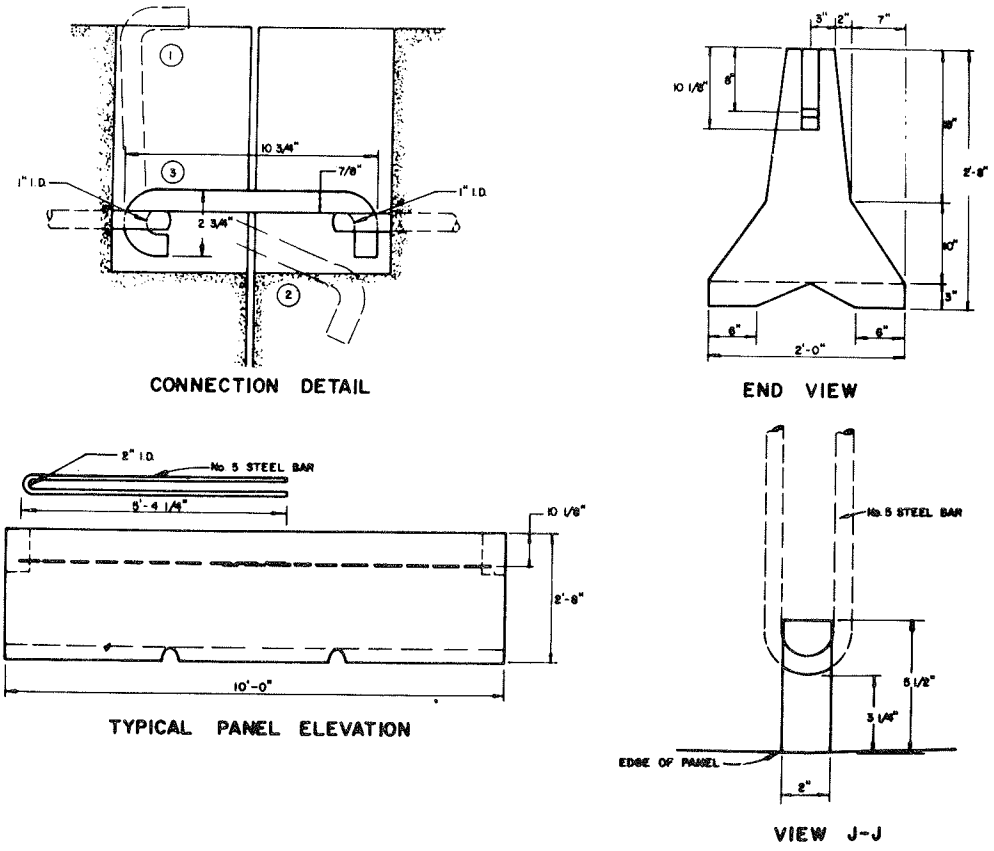

Figure 5. California pin-rebar connection.

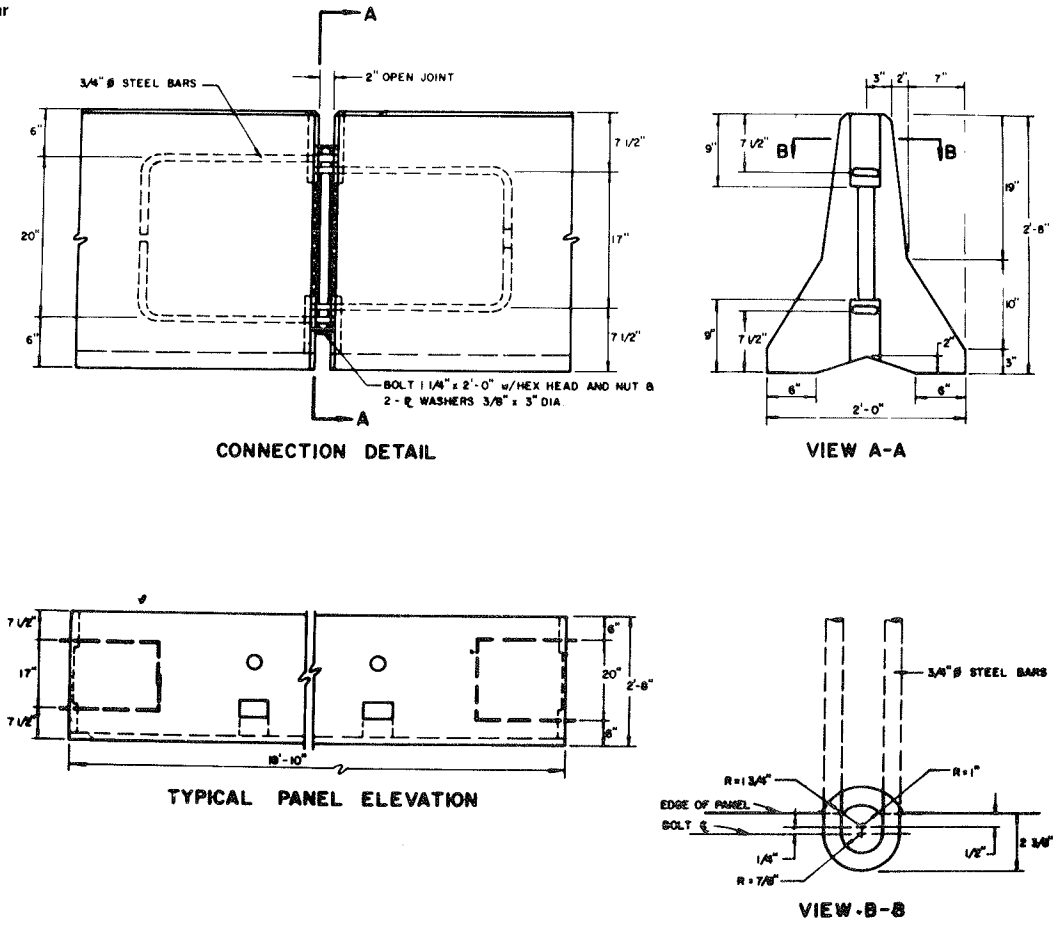

Performance Level	Condition Speed (miles/h)	Angle (°)	Weight (lb)
1	60	7	4 500
2	60	15	4 500
3	60	25	4 500
4	60	15	25 000

The tests conducted to date indicate that certain barrier designs are capable of performing at certain levels. Figure 10 implies that the 3.81-m (12.5-ft) barrier tested in Caltrans test 291 will meet performance level 1, the 6.10-m (20-ft) barrier tested in Caltrans test 294 will meet performance level 2, and several other designs, including the New York and SwRI 6.10-m designs and the TTI 9.14-m

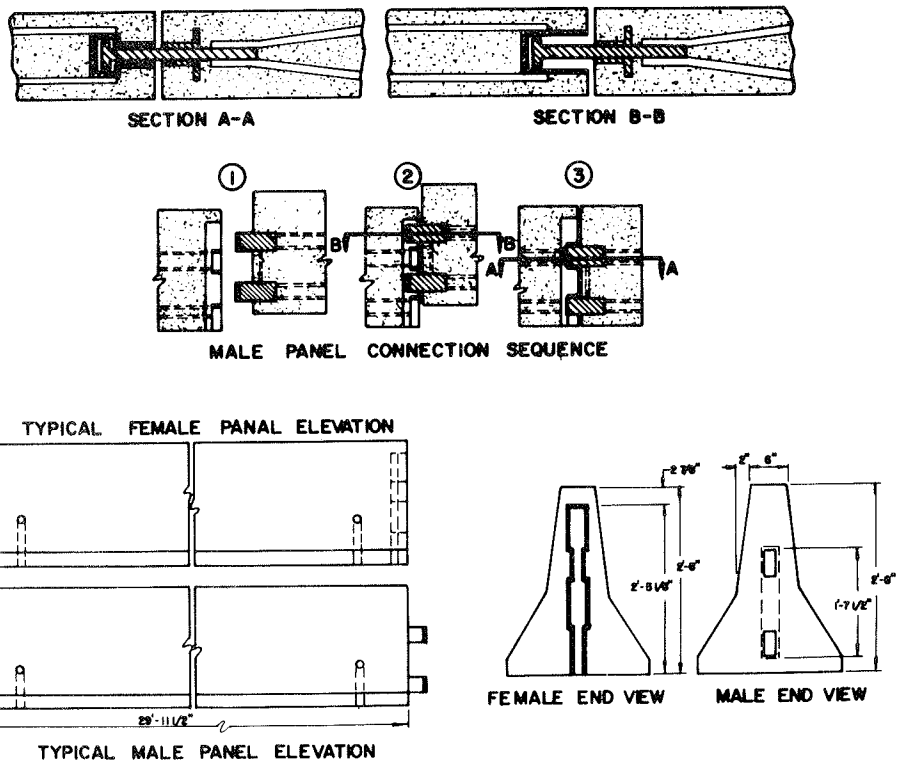

Figure 6. New Jersey Welsbach interlock connection.

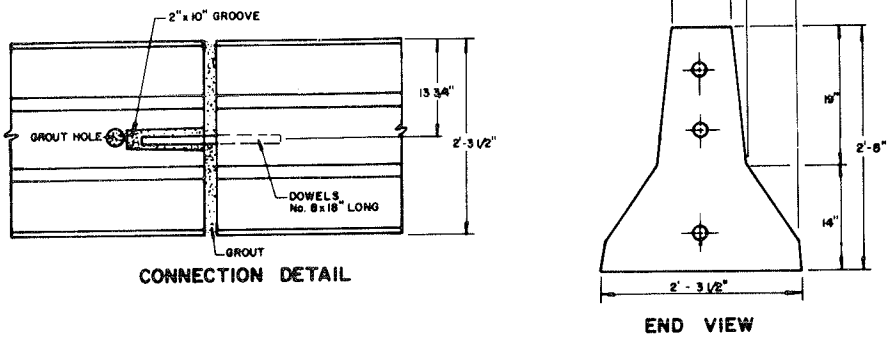

Figure 7. Texas dowel connection.

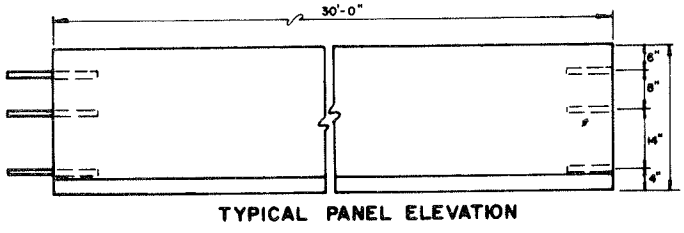

Figure 8. New York "CI" interlock.

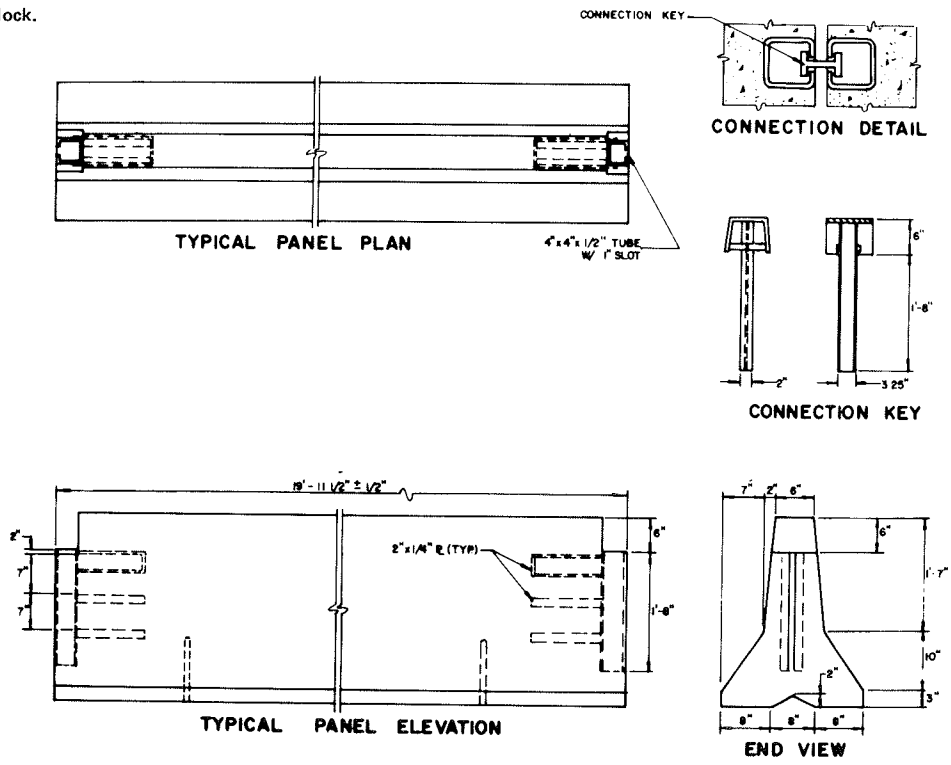

Table 1. Results of tests of portable CMBs.

Testing Agency	Test No.	Condition: Speed (miles/h)	Condition: Angle (°)	Condition: Weight (lb)	Length (ft)	Type of Connection	Moment (kip·ft)	Deflection (ft): Observed	Deflection (ft): Computed
Caltrans	291	65	7	4860	12.5	0.875-in pin	9	0.52	0.18
	292	68	28	4860	12.5	0.875-in pin	9	NA[a]	–
	293	66	40	4860	20	1-in pin	12	NA[a]	–
	294	39	25	4700	20	1-in pin	12	0.46	0.53
SwRI	CMB-18	62	25	4500	20	Vertical concrete key connection,	6	NA[a]	–
	CMB-24	56	24	4500	20	0.25-in plates	6	3.42	4.6
NYSDOT	NY-1	53	25	4250	20	CI[b] (open)	96	1.33	2.19
	NY-2	58	25	4230	20	CI[b] (grouted)	96	0.92	0.64
TTI	CMB-2	60	24	4540	30	Dowel (grouted)	50	1.1	0.89

Notes: 1 mile = 1.6 km; 1 lb = 0.45 kg; 1 kip·ft = 1.356 kN·m; 1 ft = 0.3 m.
The Welsbach design included in Table 2 was not included here because the tests conducted used a grout bed and dowels, which precluded displacement of the barrier. The barrier would thus qualify as a rigid system and might be better considered a permanent installation.

[a] Barrier segments and/or joints failed, and this precluded the structural integrity required in order for the barrier deflections to be compared with the theoretical deflections. The deflections were thus deemed not applicable.
[b] The steel member embedded in the end of the section has a C-shaped cross section, and the member that slips into the C-shaped section is I-shaped.

(30-ft) design, will meet performance level 3. Stoughton and others (4) have shown that deflections on the order of 0.6 m (2 ft) and greater lead to vehicle ramping and/or straddling of the barrier, although the end result may be containment. There is no general agreement on whether this performance meets the performance criteria of Transportation Research Circular 191 (5). California engineers have taken a conservative view that it may not and have recommended against the use of barriers that deflect to this degree, at least for permanent installations. Another view is that ultimate containment may be sufficient, even though a certain amount of straddling may take place during the impact, and that barrier integrity is the main point of the 2041-kg, 96.56-km/h (4500-lb, 60-mile/h), 25° test.

The data given in Table 3 on the specific tests as defined by barrier length and joint capacity illustrate compliance with certain performance levels. Although no barrier has been shown by test to meet performance level 4, it is speculated, based on a comparison of New York test CMB-2 and SwRI test CMB-24, that the New York "CI" joint design (Table 1) with a 6.10-m (20-ft) segment length will result in a barrier that would sustain a 15°, 96.56-km/h (60-mile/h) impact by a school bus, the arbitrary definition of performance level 4. It is noted that the New York design tested with a 2041-kg vehicle at 96.5 km/h and 25° resulted in 28 cm (11 in) of barrier deflection. When the energy level is doubled, from level 3 to level 4 [131.9-275.3 kN·m (97.3-203 kip·ft)], the barrier deflection will be considerably greater but probably not more than 0.91 m (3 ft), assuming the joint ductility is sufficient

to develop the specified capacities at a deflection that large.

ENERGY ANALYSIS OF CMB

Some elements of this energy analysis were originally developed by Stoughton in his unpublished analysis of specific CMB tests, which contributed significantly to this research.

A portable CMB subjected to a vehicle impact at or about one of the joints between segments can be analyzed by using the energy method. The analysis is subject to a number of simplifying assumptions. An overhead view of the positions of barrier segments before and after vehicle impact is shown in Figure 11.

The major simplifying assumptions are as follows:

1. Only two segments of the barrier move.
2. The amount of vehicle kinetic energy associated with the lateral component of vehicle velocity is expended in work on the barrier and the vehicle.
3. The complex development of moment in a barrier joint can be approximated as shown in Figure 12.
4. Static and sliding friction between the barrier base and the support media can be approximated as shown in Figure 13.
5. The work done in deforming vehicle structure can be approximated by an equation derived from Figure 14.

The basic energy-balance equation to be used is

$$E\ell = Em_t + E\mu + E_c \quad (1)$$

where

- $E\ell$ = amount of kinetic energy associated with the lateral component of vehicle velocity (kip•ft);
- Em_t = total of Em_1, Em_2, and Em_3, the total work done in rotating barrier joints (kip•ft);
- $E\mu$ = work done in sliding two barrier segments through the angle ϕ (kip•ft); and
- E_c = work done in deforming the vehicle structure during impact (kip•ft) (Figure 14).

Note that

$$Em_t = Em_1 + Em_2 + Em_3 \quad (2)$$

where

Table 2. Structural characteristics of CMB connections.

Connection	Tensile Force P (kips)	Shear Force V (kips)	Moment M[a] (kip·ft)	Torsion T (kip·ft)	Rotational Connection Slack (°)
Welsbach	270	160	135	95	4
New York I-lock	115	180	96	75	10
California pin and rebar[b]	44	44	37	19	9
California cable posttension	36	20	20	10	0
Texas lapped with bolt	31	22	21	11	0
Minnesota pin and eye bolt	23	23	20	15	14
Idaho pin and wire rope	23	23	19	17	5
Georgia pin and rebar	15	15	12	11	18
Texas dowel					
Calculated	0	51	0	22	NA
As tested	60	51	50		
Oregon tongue and groove	0	41	0	12	NA
Virginia tongue and groove	0	54	0	12	NA
Colorado latch	8	6	7	0[c]	9

Note: 1 kip = 4.4 kN; 1 kip·ft = 1.356 kN·m.

[a] Moment for some segments was calculated by assuming that enough of the concrete faces developed a compressive zone of contact to provide an equal opposing force to the mechanical connection acting in tension. Concrete strength was assumed to be sufficient to develop this force, although in most cases some concrete spalling would be encountered.

[b] This design, shown in Figure 5, is not the same as the designs tested in Caltrans tests 291-294. It has been structurally upgraded in comparison with the barriers for which failures were noted during tests.

[c] Barrier tilting could unlatch this design, resulting in zero capacities in the preceding three table columns.

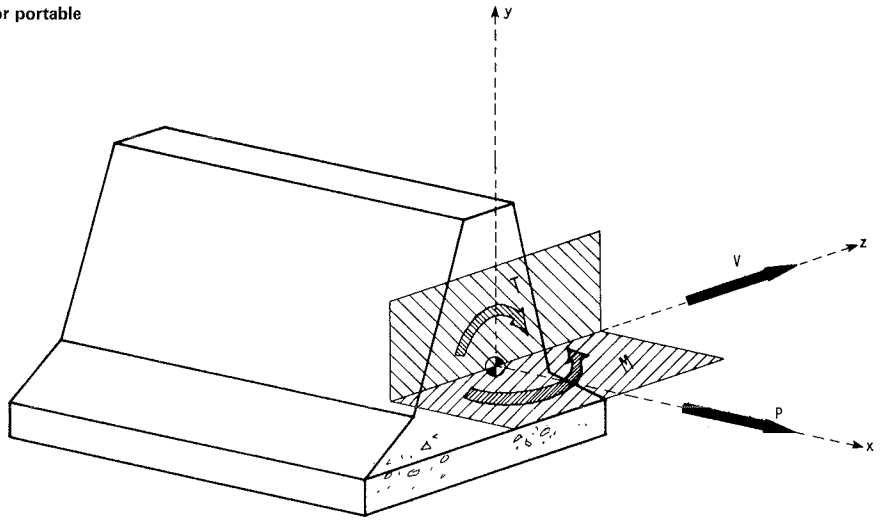

Figure 9. Coordinate system for portable CMB connection.

Em_1 = work done in rotating joint 1 through the angle ϕ (kip·ft) (Figure 12),
Em_2 = work done in rotating joint 2 through the angle 2ϕ (kip·ft) (Figure 12), and
Em_3 = work done in rotating joint 3 through the angle ϕ (kip·ft) (Figure 12).

The values of Em_1, Em_2, and Em_3 can be determined from the following integrals (or numerically from Figure 12): $Em_1 = \int_0^{\phi} M d\phi$, $Em_2 = \int_0^{2\phi} M d\phi$, and $Em_3 = \int_0^{\phi} M d\phi$, where ϕ = maximum rotation caused

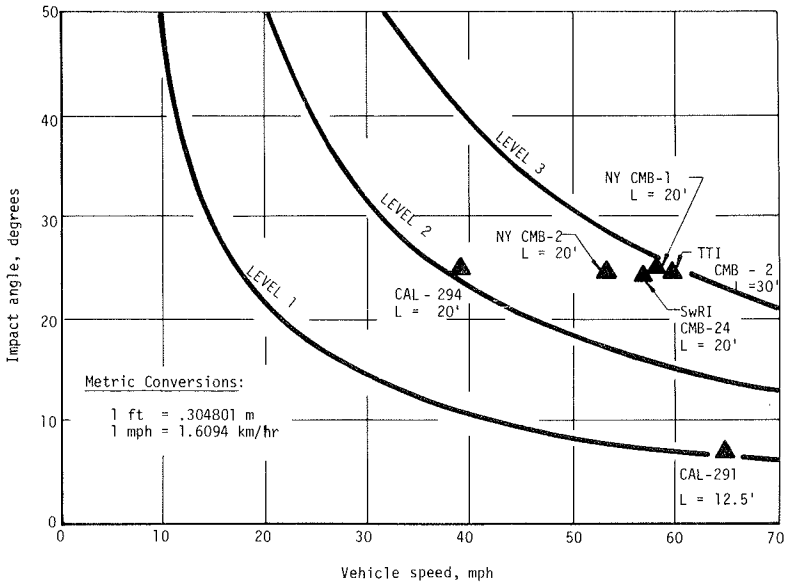

Figure 10. Functional levels related to combinations of speed and impact angle for 4500-lb automobile.

Table 3. Characteristics of portable CMBs required to meet specific functional levels.

Boundary Test Level			Joint Capacity			
Performance	Kinetic Energy[a] (kip·ft)	Segment Length[b] (ft)	Shear (kips)	Moment (kip·ft)	Torsion (kip·ft)	Deflection Limit (ft)
1	8.1	12.5	10	8	8	0.5
2	36.5	20	15	12	12	0.5
3	97.3	20	50	10	15	3.5
		30	50	50	25	3.5
4	203	20[c]	180	90	70	3[d]
		30[e]	100	100	100	2[d]

Note: 1 kip·ft = 1.356 kN·m; 1 ft = 0.3 m; 1 kip = 4.4 kN.

[a] Amount of kinetic energy related to the lateral component of vehicle velocity.
[b] For each performance level, only segment lengths whose capacities are confirmed by testing are shown.
[c] Although the appropriate function at performance level 4 of a barrier that has these capacities is unconfirmed by test, acceptable performance can probably be based on implications of NYSDOT test CMB-2 and SwRI test CMB-24.
[d] Probable.
[e] Performance shown acceptable by method of analysis described later in this paper.

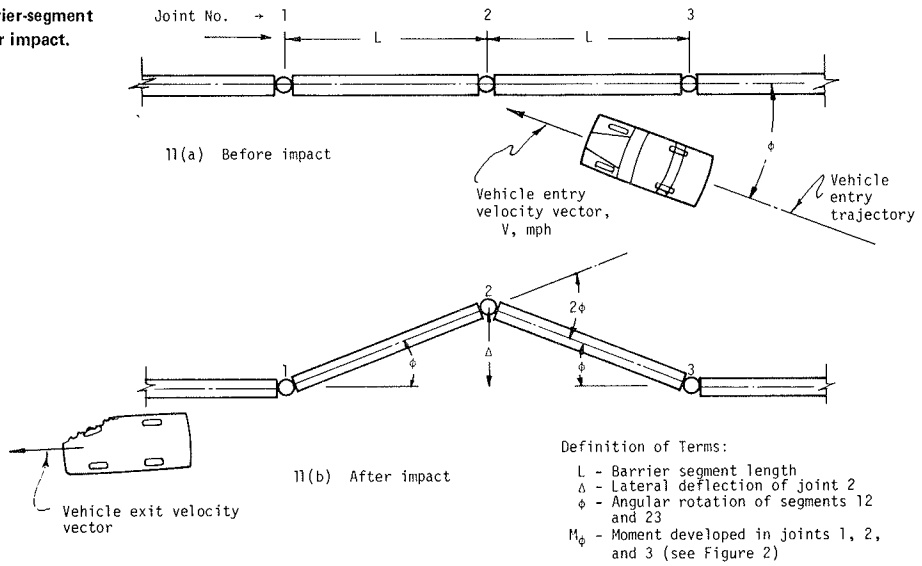

Figure 11. Idealized barrier-segment positions before and after impact.

by the impact of segments 1 and 2 and 2 and 3 (rads) and M = development of moment in a joint when it is subjected to an angular deformation of ϕ (kip•ft).

Figure 11 shows that joints 1 and 3 go through an angular deformation of ϕ while joint 2 goes through 2ϕ.

The work done in sliding the barrier segments can be computed by multiplying barrier-segment weight by the amount of friction developed in any interval of sliding movement and summing all these differential portions of work. This value is approximated by the following equation, which can be solved numerically by referring to Figure 13:

$$E\mu = WiL^2 \int_0^{\phi} u \, d\phi \tag{3}$$

where

Wi = weight per unit length of the barrier (kip/ft),
μ = coefficient of friction associated with any movement of the barrier (Figure 13), and
L = length of a barrier segment (ft).

The work done in deforming the automobile structure (E_C) is approximated by the following equation:

$$E_c = (E\ell/B_1)\{A_1 - [(A_1 - A_2) L \sin \phi]/\Delta \max\} \tag{4}$$

where A_1, A_2, and B_1 are constants used in determining E_C (kip•ft) (Figure 14) and Δmax is the maximum functional barrier deflection (ft).

By substituting the values of Em_t (Em_1 + Em_2 + Em_3), $E\mu$, and E_C into Equation 2, the following equation can be developed:

$$E\ell = (2\int_0^{\phi} M \, d\phi + \int_0^{2\phi} M \, d\phi + W_i L^2 \int_0^{\phi} \mu \, d\phi)/\left[1 - (1/B_1)\left(A_1 - \{[(A_1 - A_2) L \sin \phi]/\Delta \max\}\right)\right] \tag{5}$$

The control value of $E\ell$ is calculated from the following equation:

$$E\ell = (1/2)(W/g)(V \sin \theta)^2 \tag{6}$$

Figure 12. Joint moment versus rotation.

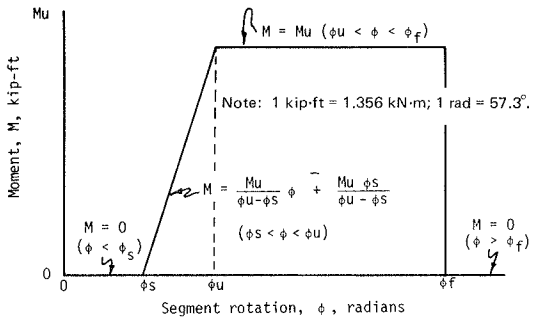

Figure 13. Barrier-support media friction versus barrier-segment rotation.

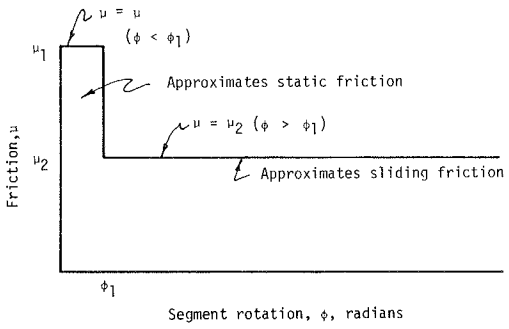

Figure 14. Estimating work done in deforming vehicle structure.

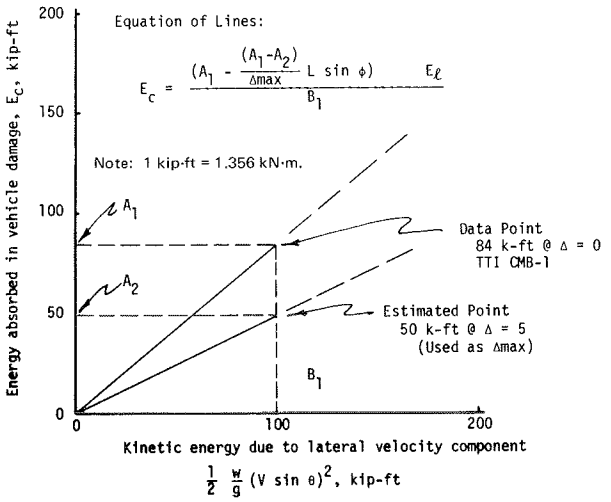

Figure 15. Flow diagram to solve for barrier deflection.

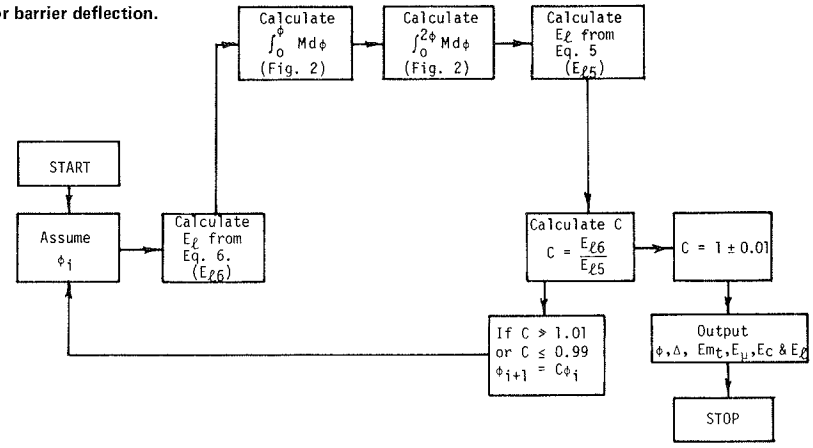

Figure 16. Computed versus observed deflections.

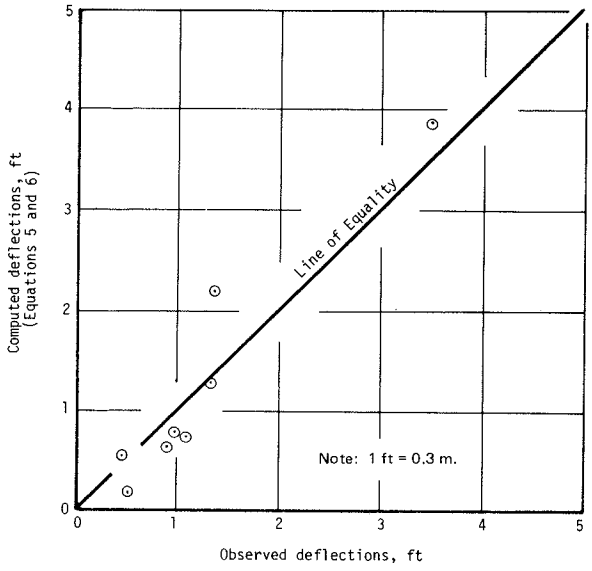

Figure 17. Lateral deflection versus connection moment.

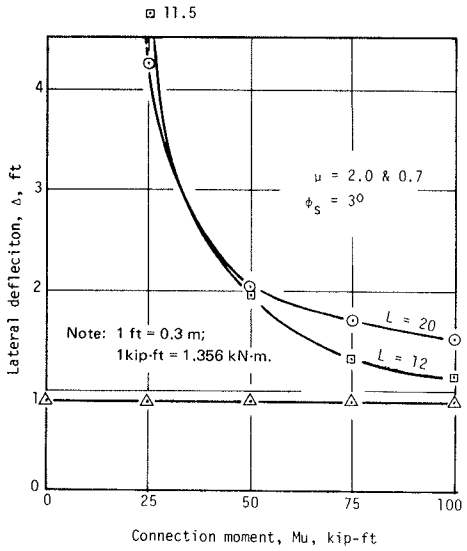

where

W = vehicle weight (kips),
g = acceleration of gravity (ft/s²),
V = vehicle velocity (ft/s), and
Θ = vehicle impact angle (°).

The solution of Equation 5 can be quickly found by using the method of finite differences: assuming a value of ϕ, calculating the value of the right side of the equation, and comparing the calculated value with the known value of Eℓ from Equation 6. If Eℓ from Equation 5 is greater than Eℓ from Equation 6, the value of ϕ is too large. A smaller value should then be estimated and the procedure repeated. If Eℓ from Equation 5 is less than Eℓ from Equation 6, the value of ϕ is too small and a larger value should be chosen for the next trial. The correct value of ϕ (i.e., the one necessary to balance the equation) will be defined within 1 percent accuracy in 10 iterations if a reasonable first estimate of ϕ is chosen. Figure 15 shows a flow chart that illustrates the determination of barrier deflection.

Figure 18. Barrier deflection versus connection slack.

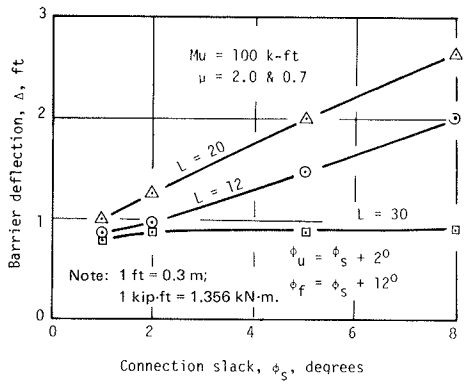

Figure 19. Lateral deflection versus barrier-segment length.

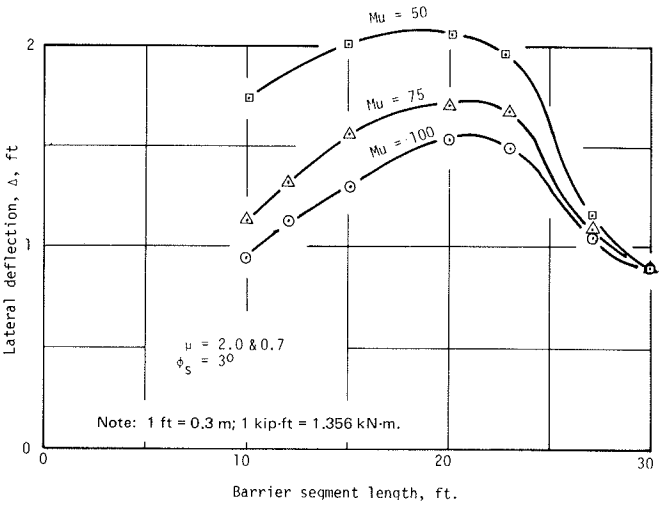

Figure 20. Lateral deflection versus equivalent static friction.

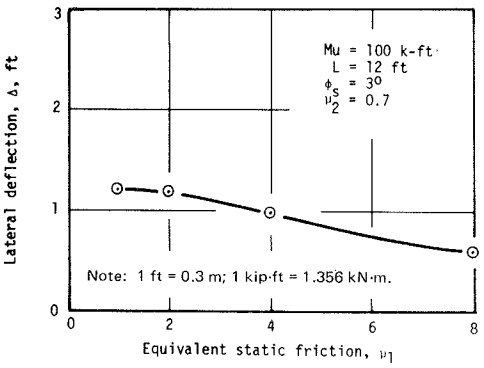

RESULTS OF ENERGY ANALYSIS

The energy analysis developed in the preceding section was performed in several different applications by using different vehicle masses, speeds, and trajectories and various barrier parameters to determine whether the analysis gave

Figure 21. Lateral deflection versus sliding friction.

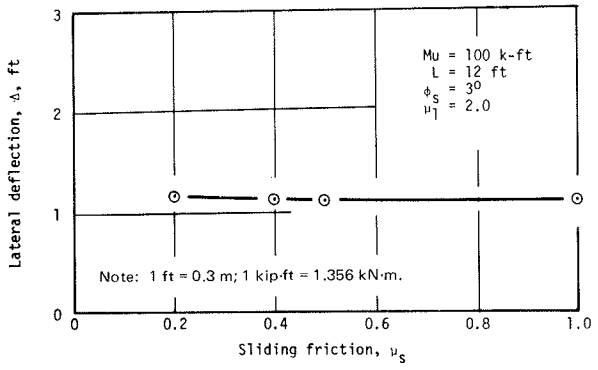

Figure 22. Barrier deflection versus barrier weight.

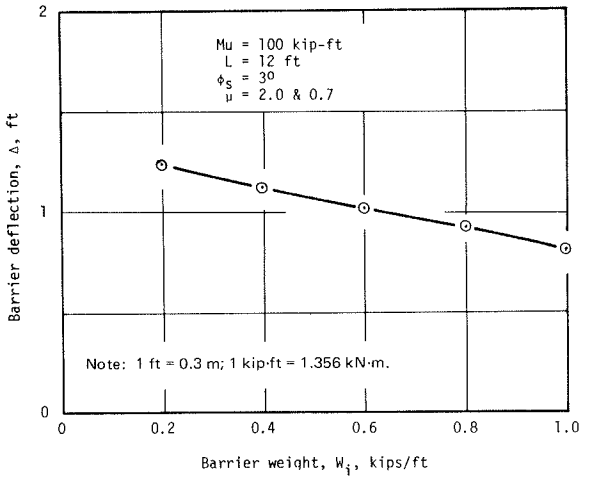

reasonable results. That exercise was considered successful. The next step in checking this solution was to compare the results of the analysis with the results of actual crash tests. The six tests that were considered applicable for comparison were Caltrans tests 291 and 294, NYSDOT tests 1 and 2, SwRI test CMB-24, and TTI test CMB-2.

Table 1 compares deflection values observed in these tests with values computed by the analytic method. Figure 16 shows that a reasonable correlation is achieved. It was further indicated by the analytic method that the speculated performance of a 6.10-m (20-ft) segment length with a 122-kN•m (90-kip•ft) ultimate moment would be inadequate at an energy level corresponding to performance level 4 [a school bus impacting at 15° and 96.6 km/h (60 miles/h)]. The analysis does indicate that a 9.14-m (30-ft) long barrier segment with a moment capability corresponding to the Welsbach joint design [184.4 kN•m (136 kip•ft)] would perform adequately at performance level 4. The barrier is predicted to deflect approximately 0.61 m (2 ft) during the school-bus impact. Based on comparisons with a fairly small number of tests, it appears that the energy analysis gives reasonable, if perhaps slightly conservative, results. At the higher levels of kinetic energy, the analysis gives deflections slightly greater than those observed in tests.

Parametric studies were conducted to determine, for the first time, barrier sensitivity to the following characteristics: connection moment capacity, barrier length, connection slack, barrier mass, and barrier-to-ground friction.

Figure 17 shows a fairly low sensitivity to connection moment between 67.8 and 135.6 kN•m (50 and 100 kip•ft) for segment lengths of 3.66 or 9.14 m (12 or 30 ft). When connection moments are less than 67.8 kN•m, sensitivity increases (deflection increases rapidly) between 33.9 and 67.8 kN•m (25 and 50 kip•ft) for barrier lengths of 3.66 and 6.10 m (12 and 20 ft). Barrier segments 9.14 m (30 ft) long are not very sensitive to connection moment at the level 3 test conditions.

Sensitivity to connection slack--that is, the amount one segment can rotate with respect to an adjacent segment before significant yaw moment is produced--lessens as segments become longer. Figure 18 shows an increase in deflection from 0.30 to 0.61 m (1-2 ft) as connection slack goes from 2° to 8° for a segment length of 3.66 m (12 ft); for a 9.14-m (30-ft) segment length, this sensitivity is reduced to an increase of only 14 percent [0.21-0.27 m (0.7-0.9 ft)] as connection slack increases from 2° to 8°.

A fascinating, if perhaps predictable, phenomenon occurs when the influence of barrier-segment length is determined for different values of connection moment capacity. Figure 19 shows that barrier deflection first increases with segment lengths up to a maximum of about 6.10 m (20 ft) and then decreases for segment lengths longer than 6.10 m. This phenomenon becomes less pronounced for smaller values of moment capacity and disappears entirely for a zero moment capacity. At zero moment capacity, deflection becomes continuously smaller as segment lengths increase. The reason for this is the conflicting influences of moment capacity and friction. When joint moment capacities are high, the influence of relatively large joint rotations at fairly small deflections produces significantly higher energy absorption for short segment lengths. In contrast, as segments become longer--6.10-9.14 m (20-30 ft)--the joint rotation at a given deflection becomes smaller and the influence of barrier energy absorption attributable to friction becomes dominant.

The influence of static and sliding friction on barrier deflection is shown in Figures 20 and 21, respectively. The influence of positive connection techniques, such as the dowels provided by California on some temporary installations, can be accommodated by selecting an appropriately high value of static friction. The influence of barrier mass, although perhaps academic at this stage, is shown in Figure 22. It is possible to increase the mass of portable CMBs by using heavyweight aggregate, but this is not likely to be economically justified.

At this stage, the energy analysis appears to be a useful tool in predicting barrier structural capacities. It cannot, however, predict vehicle response. This must be inferred from actual test data. Nor does it predict whether connections have the necessary shear or torsion characteristics to avoid the development of structural discontinuities. Fortunately, these requirements can be determined by standard analytic methods once barrier lateral deflection is accurately predicted.

SUMMARY AND CONCLUSIONS

Portable CMBs used in construction zones throughout the United States exhibit a wide range of structural details and performance characteristics. In many cases, designs are fabricated and applications made on the assumption of adequate performance. Of primary importance is the fact that there has not been a reliable analytic method by which to design

these barriers. The information and analyses included here allow the following conclusions:

1. Some portable CMBs in use have significantly restricted performance capacity.
2. Portable CMBs can be designed to resist high-intensity vehicle impacts.
3. The energy analysis presented here is a relatively simple and useful tool in the design of portable CMBs. This analysis indicates the following: (a) Connection yaw moment capacity is critical if barrier deflections are held to reasonable levels; (b) slack in barrier connections increases barrier deflection significantly; (c) for barriers with significant yaw moment capacity, the 6.10-m (20-ft) segment length is the least effective in reducing barrier deflection; (d) increasing static barrier support friction will significantly reduce barrier deflection; and (e) over a practical range of values, barrier sliding friction has little effect on barrier deflection.

ACKNOWLEDGMENT

This paper resulted from work conducted for the Federal Highway Administration (FHWA) by the Texas Transportation Institute and the Texas A&M Research Foundation. We are grateful for the support and contributions of FHWA contract manager Morton S. Oskard and for the cooperation of highway engineers in state transportation agencies throughout the United States. We also appreciate the enthusiasm and contributions of F.J. Tamanini. The earlier work of R.L. Stoughton, which suggested some elements of the energy analysis reported here, is gratefully acknowledged.

The contents of this paper reflect our views, and we are responsible for the facts and accuracy of the data presented. The contents do not reflect the views or policies of the Federal Highway Administration. This report does not constitute a standard, specification, or regulation.

REFERENCES

1. M.E. Bronstad and C.E. Kimball, Jr. Temporary Barriers Used in Construction Zones. Southwest Research Institute, San Antonio, Task Rept., Dec. 1977.
2. T.J. Hirsch and E.L. Marquis. Crash Test and Evaluation of a Precast Concrete Median Barrier. Texas Transportation Institute, Texas A&M Univ., College Station, Rept. 223-1, Oct. 1975.
3. D.M. Parks and others. Vehicular Crash Tests of Unanchored Safety-Shaped Precast Concrete Median Barrier with Planned End Connections. California Department of Transportation, Sacramento, Aug. 1976.
4. R.L. Stoughton and others. Vehicular Impact Tests of Precast Concrete Median Barriers with Corrugated Ends and Tensioned Cables. California Department of Transportation, Sacramento, June 1978.
5. Recommended Procedures for Vehicle Crash Testing of Highway Appurtenances. TRB, Transportation Research Circular 191, Feb. 1978.

Publication of this paper sponsored by Committee on Safety Appurtenances.

Evaluation of the Performance of Portable Precast Concrete Traffic Barriers

FRANK N. LISLE AND BRADLEY T. HARGROVES

An evaluation of the portable precast concrete traffic barrier as a device for separating high-speed vehicle traffic and construction activities is presented. The evaluation included (a) a review of the literature on the performance of concrete "safety shape" barriers and (b) an examination of traffic operations and safety characteristics in a construction zone where the portable barriers were used. The literature review revealed that in using the barrier (a) the end of the barrier should never be exposed to oncoming traffic; (b) the barrier joints must be tight for the barriers to act as a system; (c) the longitudinal axis of the barriers should be placed parallel to the roadway, except when the barrier system is started with a flare; and (d) the barrier system must have lateral support to prevent vehicle penetration. For conditions at the study site, it was found that (a) there was an average of 49 vehicle contacts with the barrier for every reported accident in which the barrier was involved; (b) there was a definite tendency for motorists to stay out of the barrier lane, but avoidance of the barrier lane decreased as volume increased; and (c) with an 88-km/h (55-mile/h) posted speed limit, vehicle speeds were reduced only slightly when the barriers were in place.

This paper summarizes the results of a study requested in August 1976 by the Virginia Department of Highways and Transportation to evaluate the performance of the portable precast concrete traffic barrier (PCTB) used to separate freeway traffic and construction activities in the widening of the Virginia Beach-Norfolk Expressway (1). The evaluation consisted of (a) a review of the literature on the performance of concrete "safety-shape" barriers and (b) an examination of traffic-safety and traffic-operations characteristics during the widening of the Virginia Beach-Norfolk Expressway (VA-44). The literature was searched by the Highway Research Information Service of the Transportation Research Board.

The widening project on which the PCTBs were used covered the westerly 9.91-km (6.16-mile) portion of VA-44. The traffic volume on VA-44 ranges from 45 000 vehicles/day in the winter months to 95 000 vehicles/day in the summer months. The widening consisted of adding a median lane in each direction to an existing four-lane limited-access road. The widening project was divided into three sections of approximately 3 km (2 miles) each. Work on the first section was started in September 1976. As each section was completed, the PCTB units were moved to the next section. The new lanes were opened for traffic when possible, and all portions were in service by June 1978.

The PCTB units used on VA-44 had the New Jersey safety-shape profile. They were 0.61 m (24 in) wide, 0.81 m (32 in) high, and 3.66 m (12 ft) long